Association of insulin-degrading enzyme with a 70 kDa cytosolic protein in hepatoma cells

François AUTHIER*§, Pamela H. CAMERON† and Véronique TAUPIN‡

*Institut National de la Santé et de la Recherche Médicale U30, Hôpital des Enfants Malades, 75015 Paris, France, †Department of Anatomy and Cell Biology, McGill University, Montréal H3A 2B2, Québec, Canada, and ‡Synthélabo Recherche, Central Nervous System Research Department, 92220 Bagneux, France

We have investigated the biosynthesis, subcellular location and expression of insulin-degrading enzyme (IDE), a type-I peroxisomal protease, in semi-permeabilized hepatoma cells using pulse–chase experiments, non-denaturing immunoprecipitation protocols and Northern-blot analyses. In HepG2 cell lysates prepared from cells radiolabelled with Tran[^{35}S]-label, immunoprecipitated IDE was observed immediately after a 5 min pulse and subsequently declined during chase with $t_{\frac{1}{2}}$ of approx. 33 h. In addition to the 110 kDa IDE protein, a protein of 70 kDa (p70) was identified in radiolabelled immunoprecipitates when using a monoclonal anti-IDE antibody 9B12 under non-denaturing conditions. This same antibody did not recognize p70 on Western blots of whole-cell lysates nor in sequential immunoprecipitates of immunocomplex-bead eluates from anti-IDE immunoprecipitations. Likewise, cross-linking studies performed on intact HepG2 and H35 hepatoma cells *in vivo* revealed the existence of a hetero-oligomeric complex of 180 kDa in which IDE and p70 were physically associated. Digitonin-permeabilization studies in normal and ^{35}S-labelled HepG2 cells have defined a predominant association of IDE and its associated protein p70 with cytosol (supernatant); only a minor amount of the protein IDE was detected in peroxisomes (cellular pellet). Immunoprecipitation of IDE from ^{35}S-labelled cell lysates of normal and stably transfected Chinese hamster ovary cells overexpressing IDE failed to detect p70. Treatment of HepG2 cells with clofibrate, a peroxisome proliferator, resulted in a dose-dependent increase of the two human IDE transcripts of 3.6 and 3.2 kb. This effect was not accompanied by a similar change at the protein level, nor by a change in the subcellular location of the proteins IDE and p70. Based on these findings we propose that in hepatoma cells: (1) IDE mainly exists in a stable cytoplasmic pool that is unchanged in cells undergoing peroxisomal proliferation; and (2) p70 binding to IDE may serve to maintain the dual cytosolic and peroxisomal pools of IDE in a stable equilibrium.

INTRODUCTION

Insulin-degrading enzyme (IDE; EC 3.4.24.56), also called insulinase, and most recently, insulysin [1], is an evolutionarily conserved neutral thiol-metalloendopeptidase that was first postulated to be responsible for insulin proteolysis *in vivo* almost 40 years ago (reviewed in [2–4]). IDE belongs to the pitrilysin family M16 of zinc-metalloendopeptidases and contains the motif His-Xaa-Xaa-Glu-His at its active site, an inversion of the thermolysin active site [1,3]. Recently, IDE has been demonstrated to be the first example of a peroxisomal protease and so it was proposed that it be renamed PP110 (peroxisomal protease of 110 kDa) [5–7]. This subcellular location conformed to the presence of the type-I peroxisomal targeting signal (PTS), -Ala/Ser-Lys-Leu (-A/SKL), at the correct position in the deduced primary sequences of IDE [5,8]. Recently, the functional significance of peroxisome-associated IDE in degrading cleaved leader peptides of peroxisomal proteins targeted by the type-II PTS has been biochemically demonstrated [6]. Thus, the function of peroxisome-associated IDE is closely related to that of other members of the IDE family such as *N*-arginine dibasic convertase [9], mitochondrial processing peptidases [10], and homologues of IDE in chloroplast [11] and yeast [12], which all act as propeptide-processing enzymes.

In stably transfected Chinese hamster ovary (CHO) [6] and KMHL2 cells overexpressing IDE [7] most of the protein is localized to peroxisomes and, at a much lower concentration, to cytosol. Studies of the distribution of immunodetectable IDE by Western-blot analysis using rat liver fractions noted the presence of a small amount of the protein in purified peroxisomes while the majority was recovered in the cytosolic S fraction [5]. Thus despite possessing the type-I PTS as part of its primary sequence, IDE displays a dual cytoplasmic and peroxisomal location and is found to a variable extent in the cytosol [5,6]. Such a dual location for a type-I peroxisomal enzyme is unexpected since the chemical addition of the -SKL motif on to non-peroxisomal proteins leads to directing these entities into peroxisomes [13]. These observations raise the possibility that the cytoplasmic pool of IDE may exist in a stable equilibrium maintained by some as yet unknown mechanism(s) such as a cytosolic cofactor that binds to IDE and masks the type-I PTS from the PTS I import receptor which has been recently identified in humans and yeast (reviewed in [8]).

The object of our present study was to define the biosynthesis, metabolism and subcellular localization of IDE in metabolically labelled non-transfected hepatoma cells. We present new evidence for a mainly cytosolic location of IDE using digitonin-permeabilized HepG2 cells. We also report on the specific association

Abbreviations used: CHO, Chinese hamster ovary; DMEM, Dulbecco's modified Eagle's medium; DSS, disuccinimidyl suberate; GAP, GTPase-activating protein; HRP, horseradish peroxidase; hsp, heat-shock protein; IDE, insulin-degrading enzyme; p70, protein of 70 kDa; PPAR, peroxisome proliferator-activated receptor; PTS, peroxisomal targeting signal.

§ To whom correspondence and reprint requests should be addressed.

of IDE with a 70 kDa cytosolic protein in hepatoma cells which could explain the high level of retention of this type-I peroxisomal protein in the cytoplasm of this cell type. Finally, we tested whether the dual cytosolic and peroxisomal location of IDE changes during peroxisomal proliferation. Our results show that such treatment resulted in a net increase in the expression of IDE transcripts, but no major change in the level and subcellular distribution of the protease, nor in its 70 kDa associated protein.

EXPERIMENTAL

Protein determination, antibodies and materials

The protein content of isolated fractions was determined by the method of Bradford [14]. Mouse monoclonal antibody 9B12 directed against the human IDE [15], the IDE cDNA (pIDE-F1.BS plasmid) [16] and stably transfected CHO cells overexpressing IDE [16] were kind gifts from Dr. R. A. Roth (Stanford University, Stanford, U.S.A.). Rabbit polyclonal antisera against rat liver 3-ketoacyl-CoA thiolase (thiolase), rat liver hydratase dehydrogenase and the tripeptidic peroxisomal targeting signal SKL [5,6] were gifts from Dr. R. A. Rachubinski (University of Alberta, Edmonton, Canada). Rabbit polyclonal IgG (06-157) against human GTPase-activating protein (GAP) was purchased from UBI. A mixture of mouse monoclonal antibodies directed against the cytoplasmic constitutive (73 kDa) or inducible (72 kDa) heat-shock proteins (hsps) were from Dr. P. A. Walton (McGill University, Montréal, Canada) and have been described previously [17]. Horseradish peroxidase (HRP)-conjugated goat anti-(rabbit IgG or mouse IgG) antibodies were from Bio-Rad. The Enhanced ChemiLuminescence detection kit was from Amersham. Tran[^{35}S]-label and [α-^{32}P]dCTP were purchased from ICN Radiochemicals. PAGE reagents were from Boehringer Mannheim. 1,10-Phenanthroline was obtained from Baker Chemical Co. Disuccinimidyl suberate (DSS) was purchased from Pierce. Digitonin was from Calbiochem. *Eco*RI restriction enzyme and TRIzol were purchased from Life Technologies.

Cell culture

CHO cell lines were grown in Ham's F12 medium supplemented with 10% (v/v) fetal bovine serum and 1% penicillin/streptomycin in an atmosphere of 95% air/5% CO_2. For stably transfected CHO cells overexpressing IDE [6,16], 400 μg/ml G418 was added. Human (HepG2) [18] and rat (H35) hepatoma cells were grown in Dulbecco's modified Eagle's medium (DMEM) supplemented with 10% (v/v) fetal bovine serum and 1% penicillin/streptomycin in an atmosphere of 95% air/5% CO_2. Treatments were started 24 h after hepatoma cells were plated on to dishes. Clofibrate and retinoic acid were dissolved in DMSO, resulting in a final DMSO concentration of 0.2% (v/v) in the medium. Control cells received 0.2% DMSO only. Hepatoma cells were incubated in the presence of these drugs for a period of 6 days. Final clofibrate concentrations of 0.5 and 0.1 mM, and a retinoic acid concentration of 0.01 mM, previously shown in cultured hepatocytes to produce maximal induction of peroxisomal β-oxidation [19], were used in these studies.

Metabolic labelling and immunoprecipitation

Cells were preincubated in methionine-free DMEM for 1 h and then labelled at 37 °C with Tran[^{35}S]-label (100 μCi/ml) for the specified time. In pulse–chase experiments, the chase was performed by washing the cells once with DMEM followed by incubation in DMEM supplemented with 2 mM L-methionine. Cells were harvested as follows: cultures were washed three times with HBS buffer (50 mM Hepes, pH 7.5, 200 mM NaCl), scraped, and lysed in HBS buffer containing 1% Triton X-100, 0.5% deoxycholate, 1 mM PMSF, 0.5 mM 1,10-phenanthroline, 0.1 μM E64, and 10 μg/ml each of aprotinin, leupeptin and pepstatin-A. For some experiments, protease inhibitors were added to the medium during the pulse labelling or were omitted in the lysis buffer with no detectable change in the pattern of ^{35}S-labelled proteins. Clarification of the extracts was achieved by centrifugation for 30 min at 300000 g_{av}. Cell lysates were precleared with protein G–Sepharose for 30 min at 4 °C, and incubated with monoclonal anti-IDE 9B12 or anti-(hsp 72/73) antibodies for 2 h at 4 °C (dilution 1:1000 to 1:5000). Protein G–Sepharose beads were then added, and incubation at 4 °C was continued with rotation for a further 2 h. The suspension was then centrifuged at 15000 g_{av} for 3 min, the supernatant discarded, and the beads washed three times with wash buffer (50 mM Hepes, pH 7.5, 200 mM NaCl, 0.5% Triton X-100, 0.25% deoxycholate) and once with HBS.

Sequential immunoprecipitations were carried out as described by Ou et al. [18]. After immunoprecipitation under non-denaturing conditions with monoclonal antibodies as described above, proteins were eluted from the protein G–Sepharose beads under denaturing conditions by suspending the beads in 0.2 ml of HBS containing 1% SDS and heating at 90 °C for 5 min. The supernatants were then diluted with 1.5 ml of HBS containing 1% Triton X-100. After centrifugation, the supernatant was used for a second immunoprecipitation with anti-IDE 9B12 or anti-(hsp 72/73) antibodies. All immunoprecipitates were analysed on SDS/PAGE gels followed by fluorography.

Immunoblot studies

Electrophoresed samples were transferred to nitrocellulose blots (0.45 μm) for 60 min at 380 mA in transfer buffer containing 25 mM Tris base and 192 mM glycine. The blots were blocked with 5% skimmed milk in 10 mM Tris/HCl, pH 7.5, 300 mM NaCl and 0.05% Tween-20 for 3 h. The blots were incubated with primary antibody in the above buffer for 16 h at 4 °C [anti-(human IDE) 9B12 diluted 1:500, rabbit antisera against human GAP diluted 1:500, rat liver thiolase diluted 1:300, rat liver hydratase dehydrogenase diluted 1:200, and the tripeptide SKL diluted 1:500]. After incubation, the blots were washed three times in 10 mM Tris/HCl, pH 7.5, 300 mM NaCl, 0.5% skimmed milk and 0.05% Tween-20 over a period of 1 h at room temperature. The bound immunoglobulin was detected using HRP-conjugated goat anti-(rabbit IgG) for the polyclonal antibodies, or HRP-conjugated goat anti-(mouse IgG) for the monoclonal anti-IDE antibody. Quantification was done by densitometric scanning of the X-rays of corresponding immunoblots.

Permeabilization of HepG2 cells with digitonin

A modification of the procedure of Authier et al. [6] was followed. HepG2 cells were grown to subconfluent densities on 55-mm-diam. culture dishes, rinsed three times in HBS buffer and incubated with 1 ml of 20 mM sodium phosphate, pH 7.4/150 mM NaCl (PBS buffer) containing digitonin at concentrations ranging from 0.01 to 2 mg/ml. After 10 min of gentle agitation at 4 °C, the cell medium was collected; this material was referred to as the cell supernatant. A 1 ml aliquot of HBS containing 1% Triton X-100/0.5% deoxycholate and the above-specified protease inhibitors was added to each dish and the cells were scraped. Clarification of the extracts was achieved by centrifugation for 30 min at 300000 g_{av}; this cell lysate was referred to

as the cell pellet. The pellets and supernatants from non-radiolabelled HepG2 cells were evaluated by immunoblotting for their content of the cytosolic proteins GAP and pre-thiolase precursor, for their content of the peroxisomal marker enzyme thiolase, and for their content of IDE. In some experiments, HepG2 cells were metabolically radiolabelled for 2 h with Tran[^{35}S]-label prior to digitonin treatment. The radiolabelled cell pellets were evaluated for their content of IDE by immunoprecipitation with anti-IDE antibody 9B12 as described above.

Cross-linking studies

IDE was cross-linked *in vivo* to its associated 70 kDa protein (p70) in intact cells. Subconfluent hepatoma cells were washed three times with ice-cold HBS buffer, and then 3 ml of 0.3 mM DSS (stock solution at 30 mM dissolved in DMSO) in ice-cold PBS buffer was added to the 100-mm-diam. dish of cells. The procedure described above was found to cross-link the p70 protein to IDE to the greatest extent, the amount of the covalent complex not being increased by higher concentrations of DSS. Control cell cultures were exposed to PBS buffer with and without 0.5 % DMSO. After 15 min at 4 °C, the cells were washed three times with 20 mM Tris/HCl, pH 7.4, containing 150 mM NaCl, solubilized with 1 ml of lysis buffer (20 mM Tris/HCl, pH 7.4, 1 % Triton X-100, 0.5 % deoxycholate, 1 mM PMSF, 0.5 mM 1,10-phenanthroline, 0.1 μM E64, 10 μg/ml each of aprotinin, leupeptin and pepstatin-A). After centrifugation for 30 min at 300000 $\boldsymbol{g}_{av}$, the cell lysates were analysed by Western blots using anti-IDE antibody 9B12. In some experiments, HepG2 and H35 cells were metabolically radiolabelled for 2 h with Tran[^{35}S]-label prior to cross-linking experiments. The radiolabelled cell lysates were immunoprecipitated using anti-IDE antibody 9B12 as described above.

RNA isolation and Northern blotting

The same number of cells (1×10^6) were seeded in 100-mm-diam. dishes, and 24 h later cells were treated or not with various drugs as described above, and grown to 70–80 % confluency. After one washing step with HBS, total RNA were extracted by the acid guanidinium thiocyanate–phenol–chloroform method using TRIzol. The *Eco*RI restriction fragment of IDE cDNA was isolated by electrophoresis through a 1 % agarose gel, removal of the appropriate band and purification using Qiaex (Qiagen). The 3.0 kb *Eco*RI restriction fragment of IDE cDNA (25 ng) and a cDNA β-actin probe were labelled with [α-^{32}P]dCTP (5 μCi) using a random primer labelling kit (Life Technologies). RNA (20 μg) was electrophoresed through a 1 % agarose gel containing formaldehyde and transferred to nylon membranes (Hybond-N, Amersham). RNA samples were cross-linked to the membranes using the Stratalinker (Stratagene) UV cross-linking apparatus. Filters were prehybridized for 1–4 h at 42 °C in 50 % formamide/1 M NaCl/1 % SDS/10 % dextran sulphate/50 μg/ml denatured fragmented salmon sperm DNA. Hybridization was performed overnight at 42 °C with ^{32}P-labelled cDNA probes in the same solution. Blots were washed twice with 1 × SSC (0.15 M NaCl/0.015 M sodium citrate) for 15 min at room temperature, with 0.1 × SSC containing 0.1 % SDS for 15 min at room temperature and 0.1 × SSC containing 0.1 % SDS for 30 min at 65 °C. Filters were then exposed to Kodak XAR-5 film for 1–4 days at −80 °C. Quantification of the radioactivity of the hybridized probe was carried out using a BAS 2000 Fuji Bio-Imaging Analyser (Fuji BioMedical Systems, Inc., Bethesda, MD, U.S.A.).

RESULTS

We have attempted to understand the significance of the dual cytosolic and peroxisomal distribution of IDE in liver parenchymal cells by: (i) defining the turnover rate of the protease in hepatoma cells using pulse–chase experiments; (ii) characterization of a cofactor that binds to IDE in hepatoma cells using non-denaturing immunoprecipitation and affinity cross-linking procedures; and (iii) assessment of the distribution and expression of the protein IDE and its mRNA in HepG2 cells undergoing peroxisomal proliferation.

Synthesis and turnover rate of IDE in metabolically labelled hepatoma cells

To examine the cellular metabolism of IDE, HepG2 cells were metabolically radiolabelled with Tran[^{35}S]-label, and IDE was recovered from cell lysates by immunoprecipitation using anti-IDE antibody 9B12 (Figure 1). In Figure 1(A), HepG2 cells were pulse-labelled for 5 min to 2 h. Newly synthesized IDE was clearly discernible as a 110 kDa band after 5 min (lane 1) and the amount of radiolabelled IDE increased over the 2 h pulse period (lanes 2–5). To estimate the turnover rate of IDE HepG2 cells were pulse-labelled for 2 h and chased for various times (Figure 1B). While a slight increase in the amount of radiolabelled IDE was observed after 1 h chase (lane 2), this gradually declined over the next 44 h (lane 4) to 15 % of that observed at the start of the chase period (lane 1). This allowed us to estimate the half-life of cellular IDE to be approx. 33 h.

In addition, a 70 kDa protein (p70) was detected in the fluorograph of the IDE-immunoprecipitates. This 70 kDa band did not appear immediately, but only after 30 min of radiolabelling (Figure 1A, lanes 3–5). During the chase period (Figure 1B), the disappearance of radiolabelled p70 was concomitant with that of radiolabelled IDE, suggesting that the two proteins were associated.

Evidence for the specific association between IDE and p70 in hepatoma cells

Two experiments were carried out to show that the anti-IDE antibody 9B12 selectively recognizes only IDE. First, Western-blot analysis of equal amounts of protein from total cell lysates isolated from HepG2 (Figure 2A, lane 1) and H35 hepatoma cells (Figure 2A, lane 2) using anti-IDE antibody 9B12 indicated the presence of a single antigenic protein of apparent molecular mass 110000 Da. No detectable immunoreactivity was found in other regions of the blot.

Next, HepG2 cells were labelled with Tran[^{35}S]-label for 2 h, and cell lysates were immunoprecipitated with anti-IDE antibody 9B12 (Figure 2B, lane 1). The IDE immunoprecipitate was then eluted from the protein G–Sepharose beads by incubating the beads in SDS-containing buffer and re-immunoprecipitated with anti-IDE antibody 9B12 (Figure 2B, lane 2). Under these conditions, re-immunoprecipitated IDE was clearly visible, whereas radiolabelled p70 was undetectable. Together, these experiments indicate that the anti-IDE antibody 9B12 selectively recognizes IDE under denaturing (Figure 2A) and non-denaturing conditions (Figure 2B).

A radiolabelled diffuse band of 80–85 kDa was also observed in the immunoprecipitate of Figure 2(B) (lane 1). This diffuse band was only observed in immunoprecipitates of lysates from cells which had been radiolabelled for 1 h or more (see Figure 1A, lanes 4 and 5) and was not consistently observed (compare with Figures 1B, 4B and 5B). In addition, the 80–85 kDa band was only prominently observed in fluorographs which had been

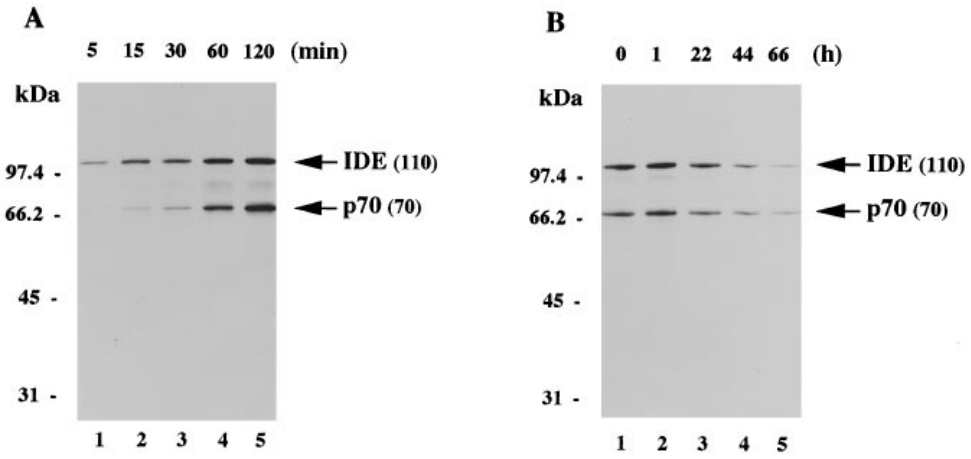

Figure 1 Time course of the association of p70 protein with IDE

(**A**) HepG2 cells were pulse-labelled with Tran[^{35}S]-label (100 μCi/ml) for 5 min to 2 h (lanes 1–5). At the indicated times, cells were lysed and immunoprecipitated with anti-IDE antibody 9B12. IDE immunoprecipitates were analysed by SDS/PAGE and fluorography. (**B**) HepG2 cells were pulse-labelled for 2 h and chased in DMEM containing 2 mM methionine for the indicated times (0 to 66 h; lanes 1–5). The arrows on the right indicate the mobility of ^{35}S-labelled IDE (110 kDa) and p70 protein (70 kDa). Identical results were obtained with rat H35 hepatoma cells (results not shown).

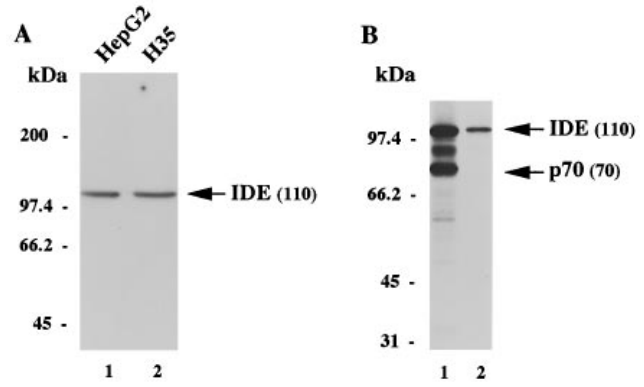

Figure 2 P70 protein is immunologically distinct from IDE

(**A**) HepG2 (lane 1) and H35 (lane 2) cell lysates (20 μg/lane) were subjected to SDS/PAGE, transferred to nitrocellulose, and immunoblotted with anti-IDE antibody 9B12. (**B**) HepG2 cells were radiolabelled for 2 h followed by lysis and non-denaturing immunoprecipitation with anti-IDE antibody 9B12 (lane 1). Co-precipitated proteins were eluted from protein G–Sepharose beads with SDS. Sequential immunoprecipitation was done with anti-IDE antibody 9B12 followed by SDS/PAGE and fluorography (lane 2).

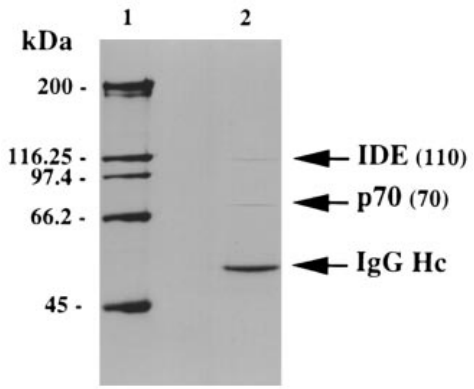

Figure 3 Purification of p70 protein by co-immunoprecipitation from non-radiolabelled HepG2 cell lysates

HepG2 cells were grown to subconfluent densities, washed, lysed and immunoprecipitated with anti-IDE antibody 9B12. IDE immunoprecipitate was then subjected to SDS/PAGE. The distribution of co-immunoprecipitated proteins (lane 2) is shown by staining with Coomassie Brilliant Blue and compared with the mobilities of molecular mass markers (lane 1).

subjected to prolonged autoradiography exposures. Its identity is unknown but may correspond to partially degraded IDE.

A co-immunoprecipitation purification protocol was also used to examine the association of IDE and p70 (Figure 3). Following non-denaturing immunoprecipitation of IDE from non-radiolabelled HepG2 cell lysates, evaluation by SDS/PAGE of immunoprecipitated proteins showed two Coomassie Blue-stained proteins of 110 kDa (the IDE protein) and 70 kDa (the p70 protein), as well as the immunoprecipitating IgG heavy chain (Figure 3, lane 2).

To test whether the association between IDE and p70 occurs *in vivo* in intact cells, H35 (Figure 4A) and HepG2 cells (Figure 4B) were labelled with Tran[^{35}S]-label, incubated with the bi-functional cross-linker DSS, washed, lysed, and IDE was immunoprecipitated with anti-IDE antibody 9B12. In addition to the major IDE and p70 bands, a weak band of approx. 180 kDa was observed (Figures 4A and 4B, lanes 3). The intensity of the 180 kDa band was less prominent than those of the 110 and 70 kDa bands due to a low efficiency of coupling probably related to poor diffusion of the cross-linker inside the cell. This could explain why the molar ratio of IDE to p70 observed by Coomassie Blue staining (see Figure 3) was greater than the relative intensity by which both proteins were observed to be cross-linked. However, the presence of this 180 kDa band was specifically dependent on the addition of cross-linker since the cross-linked complex was not present in control precipitates containing buffer alone (Figures 4A and 4B, lanes 1) or buffer plus DMSO (lanes 2). To test whether IDE was present in the 180 kDa cross-linked complexes, proteins from non-radiolabelled

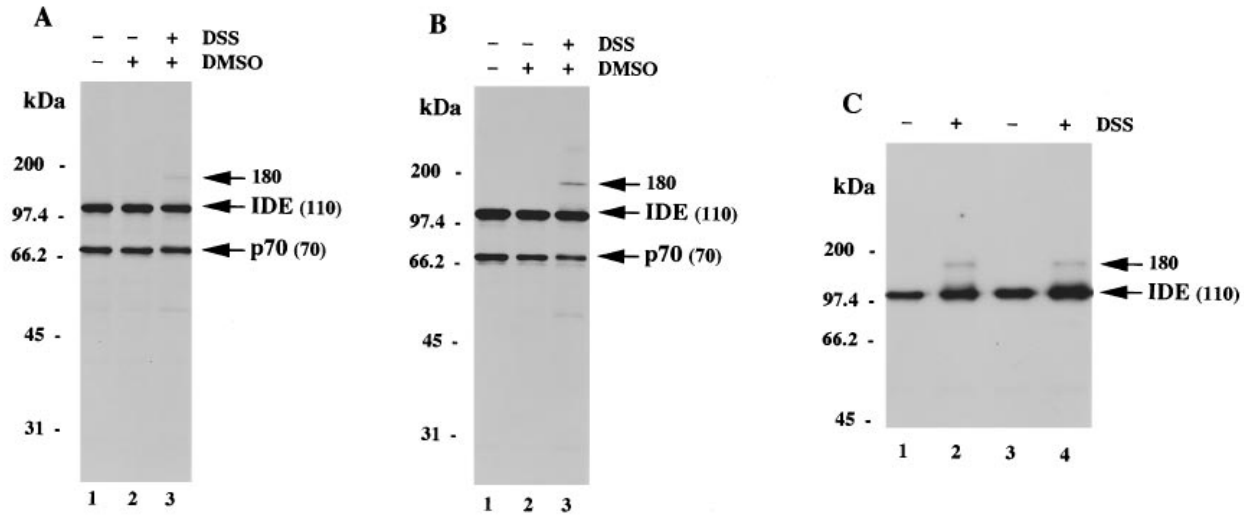

Figure 4 ***In vivo*** **cross-linking of IDE to p70 protein**

H35 (**A**) and HepG2 cells (**B**) were pulse-labelled with Tran[^{35}S]-label for 2 h. Intact cells were then incubated with buffer alone (lanes 1), with buffer containing 0.2% DMSO (lanes 2) or with 0.3 mM DSS cross-linker dissolved in buffer containing 0.2% DMSO (lanes 3), washed and lysed. Immunoprecipitates of IDE were analysed by SDS/PAGE followed by fluorography. (**C**) H35 (lanes 1 and 2) and HepG2 cells (lanes 3 and 4) were treated with DSS (lanes 2 and 4) or with buffer containing 0.2% DMSO (lanes 1 and 3), washed and lysed. The cell lysates (50 μg of protein) were subjected to SDS/PAGE, transferred to nitrocellulose and immunoblotted with anti-IDE antibody 9B12. The mobility of the cross-linked complexes ($\approx$180 kDa) is indicated by the arrows on the right.

H35 (Figure 4C, lanes 1 and 2) and HepG2 cell lysates (Figure 4C, lanes 3 and 4) were analysed on Western blots with the anti-IDE antibody 9B12. Cells treated with DSS (lanes 2 and 4) but not control cells (lanes 1 and 3) exhibited an immunoreactive band at 180 kDa as well as the more abundant 110 kDa IDE band.

Members of the cytosolic hsp70 family have been demonstrated to be involved in the import of proteins into the lumen of the mammalian peroxisome [17]. To test whether p70 was hsp70, HepG2 cells were radiolabelled and cell lysates immunoprecipitated with anti-IDE 9B12 antibody under non-denaturing conditions, followed by sequential immunoprecipitation using a mixture of monoclonal anti-(hsp72/73) antibodies [17]. No radioactive bands were observed in the sequential immunoprecipitation lanes, ruling out the possibility that p70 was hsp70 (results not shown). Finally, the possibility that p70 represents a proteolytic fragment derived from IDE was also ruled out by the absence of an effect with a diversity of protease inhibitors (see the Experimental section) on the ^{35}S-labelling pattern when compared with experiments omitting these inhibitors. Additional control experiments were extended incubations of radiolabelled cell lysates prepared in the absence of protease inhibitors and incubated *in vitro* at 37 °C before assessment by SDS/PAGE analysis, with no detectable change of p70 level relative to IDE (results not shown).

Subcellular location of IDE and p70 protein in digitonin-permeabilized hepatoma cells

A digitonin-permeabilized cell system was developed and used to characterize the intracellular distribution of IDE and its associated protein p70 (Figure 5). The loss of cytosolic and peroxisomal content was examined by measuring the amount of immunodetectable GAP and pre-thiolase precursor (cytosolic markers), and mature thiolase (peroxisomal marker) in both the semi-permeabilized cells (cellular pellet) and the digitonin-soluble extracts (supernatant) (Figure 5A). More than 95% of cytosolic GAP was released at the digitonin concentration of 0.1 mg/ml (supernatant; lane 5), while peroxisomal thiolase was undetectable in this supernatant fraction. The release pattern of IDE was essentially the same as that of the cytosolic marker GAP. Approx. 70% of IDE was released with the cytosolic proteins at the digitonin concentration of 0.1 mg/ml, and the rest with the peroxisomal protein thiolase at concentrations below 0.3 mg/ml. These data indicate a dual location for IDE in HepG2 cells, mainly in the cytoplasm, and partly ($< 30\%$) in peroxisomes.

Digitonin-permeabilization studies were performed on Tran[^{35}S]-labelled HepG2 cells to address the subcellular location of the protein p70 (Figure 5B). HepG2 cells were metabolically radiolabelled for 2 h, digitonin-permeabilized, pelleted, and radiolabelled cell lysates were incubated with the anti-IDE antibody 9B12. Both radiolabelled IDE and p70 proteins were released at a digitonin concentration of 0.1 mg/ml (Figure 5B, lane 5), suggesting that these newly synthesized proteins are together mainly located in the same cytoplasmic compartment.

Biosynthesis of IDE in metabolically radiolabelled CHO cells

Since stably transfected CHO cells overexpressing IDE revealed a major peroxisomal location for the proteinase [6], we have evaluated the putative presence of p70 in this cell type and compared it with non-transfected CHO cells (Figure 6). Non-transfected CHO cells (lanes 1–5) and stably transfected CHO cells overexpressing IDE (lanes 6–10) were pulse-labelled for 10 min to 2 h, and IDE was then recovered by immunoprecipitation of cell lysates using anti-IDE antibody 9B12. In agreement with a previous report [16], lysates from normal CHO cells had detectable levels of IDE expression. Newly synthesized radiolabelled IDE was only discernible after a 30 min pulse period in non-transfected CHO cells (Figure 6, lanes 3–5), whereas CHO cells overexpressing IDE showed high levels of

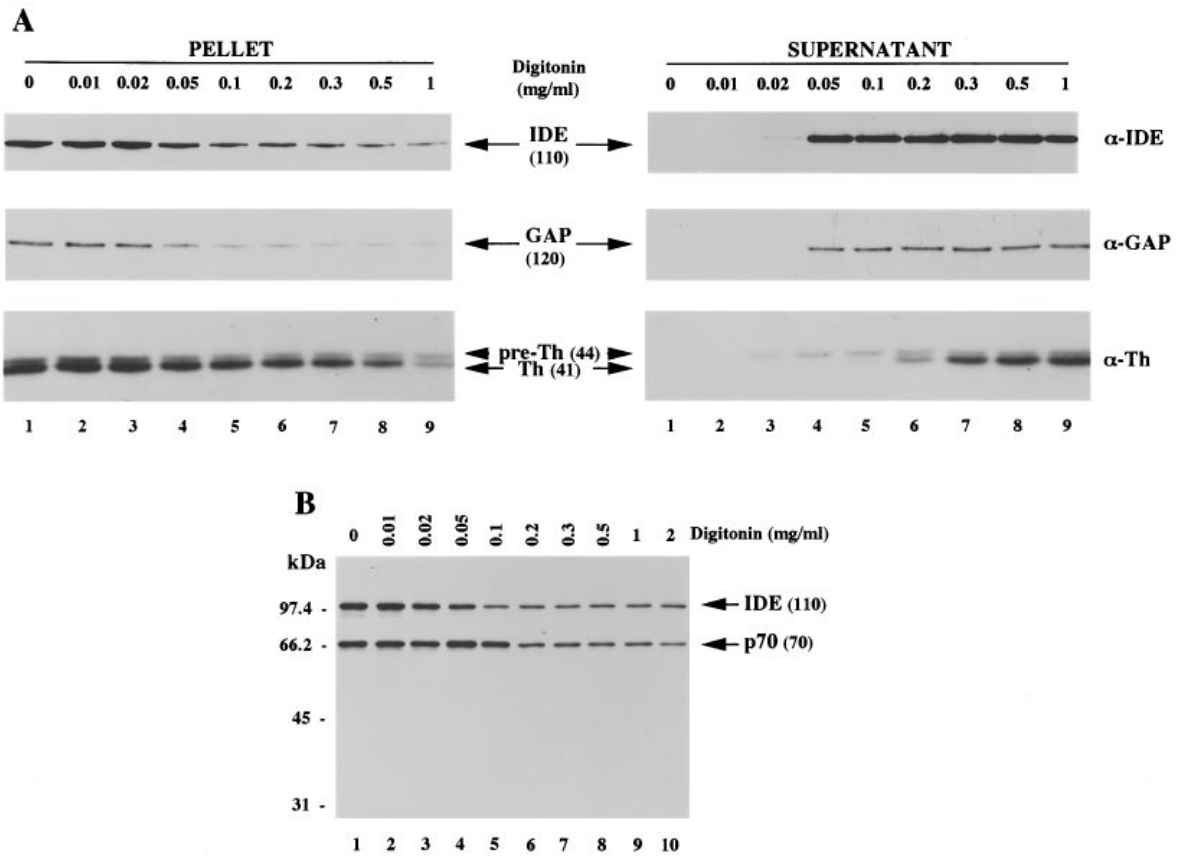

Figure 5 Major cytoplasmic localization of IDE and p70 in HepG2 cells

(**A**) Pellets and supernatants from control (lanes 1) and digitonin-treated HepG2 cells (lanes 2–9) were evaluated by immunoblotting for their content of IDE with the anti-IDE antibody 9B12; for their content of GAP with polyclonal IgG; and for their content of pre-thiolase and thiolase proteins with polyclonal antiserum. Equal volumes of pellets and supernatants were loaded on each lane of the gel. (**B**) HepG2 cells were pulse-labelled with Tran[^{35}S]-label for 2 h and then digitonin-permeabilized. Radiolabelled cell lysates from control (lane 1) and digitonin-treated cellular pellets (lanes 2–10) were immunoprecipitated with anti-IDE antibody 9B12. Immunoprecipitated proteins were analysed by SDS/PAGE followed by fluorography. Identical results were obtained with rat H35 hepatoma cells (results not shown).

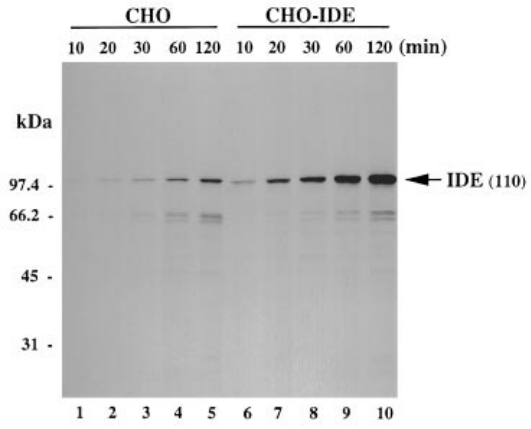

Figure 6 Metabolic labelling of IDE in non-transfected and stably transfected CHO cells overexpressing IDE

Non-transfected (lanes 1–5) and stably transfected CHO cells overexpressing IDE (lanes 6–10) were pulse-labelled with Tran[^{35}S]-label (100 μCi/ml) for 10 min to 2 h. At the indicated times, cells were lysed and immunoprecipitated with anti-IDE antibody 9B12. The arrow on the right indicates the mobility of ^{35}S-labelled IDE (110 kDa).

IDE expression immediately after a 10 min pulse (lane 6). In addition to the major radiolabelled 110 kDa IDE protein, very faint lower-molecular-mass bands were discernible in the 62 to 68 kDa region. However, none of these bands corresponded to the electrophoretic mobility or to the intensity of that of p70, the IDE-associated protein detected in HepG2 cells (compare Figure 1A with Figure 6). Moreover, the amount of these co-precipitated proteins in the anti-IDE immunoprecipitates was not dependent on the level of IDE expression since the labelling of these bands was not amplified by the overexpression of IDE. These results suggest that these co-precipitated proteins, contrary to that for p70, were not IDE-associated.

Subcellular location and expression of IDE in HepG2 cells treated with peroxisomal proliferators

Clofibrate and retinoic acid, two drugs reported to induce the proliferation of liver peroxisomes [19,20], were used on HepG2 cells to assess whether the dual cytoplasmic and peroxisomal distribution of IDE changes during peroxisomal proliferation (Figure 7). Following drug treatment HepG2 cells were digitonin-permeabilized and quantitative analysis by immunoblotting

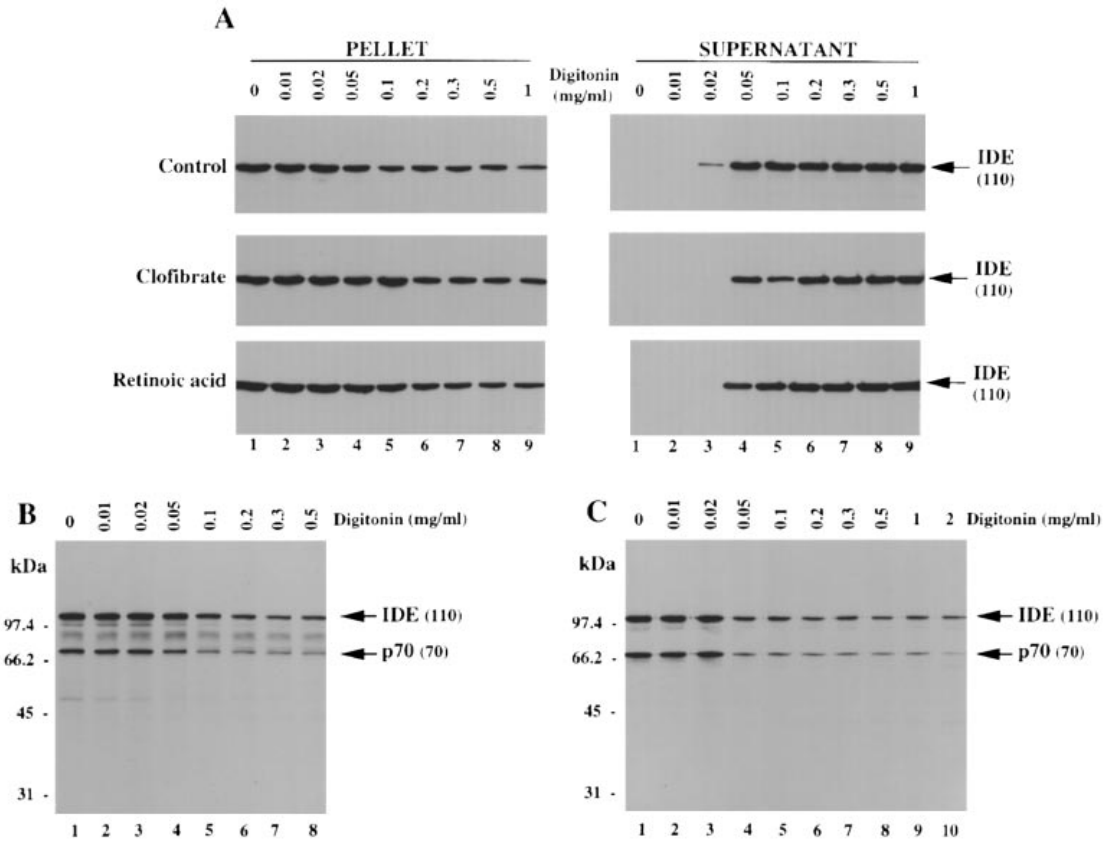

Figure 7 Effect of clofibrate and retinoic acid on subcellular location of IDE and p70 in HepG2 cells

(**A**) Cells were incubated in the presence of 0.2% DMSO (control), 0.5 mM clofibrate dissolved in 0.2% DMSO and 0.01 mM retinoic acid dissolved in 0.2% DMSO for a period of 6 days. Cells were then digitonin-permeabilized and equal volumes of pellets and supernatants from control (lanes 1) and digitonin-treated cells (lanes 2–9) were loaded on to each lane of the gel and subsequently evaluated by immunoblotting for their content of IDE with the anti-IDE antibody 9B12. Clofibrate- (**B**) and retinoic acid-treated cells (**C**) were pulse-labelled with Tran[^{35}S]-label for 2 h and then digitonin-permeabilized. Radiolabelled cell lysates from control (**B** and **C**, lanes 1) and digitonin-treated cellular pellet (**B**, lanes 2–8 and **C**, lanes 2–10) were immunoprecipitated with anti-IDE antibody 9B12. Identical results were obtained with rat H35 hepatoma cells (results not shown).

revealed identical patterns of release of IDE into supernatants and pellets of digitonin-permeabilized control, clofibrate- and retinoic acid-treated cells (Figure 7A).

Further, the release of radiolabelled IDE and its associated protein p70 was studied by immunoprecipitation with anti-IDE antibody 9B12 of radiolabelled cell lysates from the cell pellets of digitonin-permeabilized HepG2 cells treated with clofibrate (Figure 7B) or retinoic acid (Figure 7C). Neither treatment altered the major release ($> 70\%$) of either protein at the digitonin concentration of 0.1 mg/ml (Figure 7, lanes 5) and, thus, did not significantly affect IDE and p70 subcellular localizations.

Human IDE cDNA [16,21] and monoclonal antibody 9B12 directed against human IDE [15] were used to probe, respectively, IDE transcripts and IDE protein during clofibrate and retinoic acid treatments of HepG2 cells (Figure 8). Using Northern-blot analysis with an *Eco*RI fragment of the 3.0 kb human IDE cDNA [16,21], two major transcripts of 3.6 and 3.2 kb were detected (Figure 8A). A uniform and dose-dependent increase of both 3.6 and 3.2 kb transcripts occurred upon clofibrate treatment at concentrations of 0.1 mM (Figure 8A, lane 4) and 0.5 mM (Figure 8A, lane 5) compared with control cells (Figure 8A, lanes 1 and 3). However, the levels of human IDE mRNA did not significantly change after retinoic acid stimulation (lane 2). When normalized to the levels of 28 S and 18 S ribosomal RNA, there was at least a 2.5-fold induction of human IDE transcripts in HepG2 cells treated with 0.5 mM clofibrate as estimated by scanning the Northern blots with a radioanalytical imaging system (see the Experimental section). To control for the amount of RNA loaded in each lane, a photograph of the gels before blotting was systematically taken (see inset of Figure 8A). Additionally, the same membranes were hybridized with a β-actin cDNA probe (results not shown). Both methods indicated that the increased levels of human IDE transcripts in clofibrate-treated cells are not attributable to variations in loading. The observed effect of clofibrate on the amount of IDE mRNA was not reflected at the protein level, as shown in Figure 8(B). Immunoblot analysis of equal amounts of protein from lysates of HepG2 cells which received the same treatments as in Figure 8(A) revealed no major change in the IDE protein level in clofibrate (lanes 4 and 5) and retinoic acid-treated cells (lane 2). Densitometric quantification of the immunoblots in four different experiments only revealed a slight (1.43 ± 0.19-fold) increase in IDE protein level for the 0.5 mM clofibrate concentration.

The effects of clofibrate and retinoic acid on the induction of type-I and -II peroxisomal enzymes was assessed by immunoblot analysis (Figure 9). Clofibrate-treated cell extracts revealed ≈ 2-fold increased levels of peroxisomal β-oxidation enzymes such as hydratase dehydrogenase (Figure 9A, lane 3) and thiolase (Figure

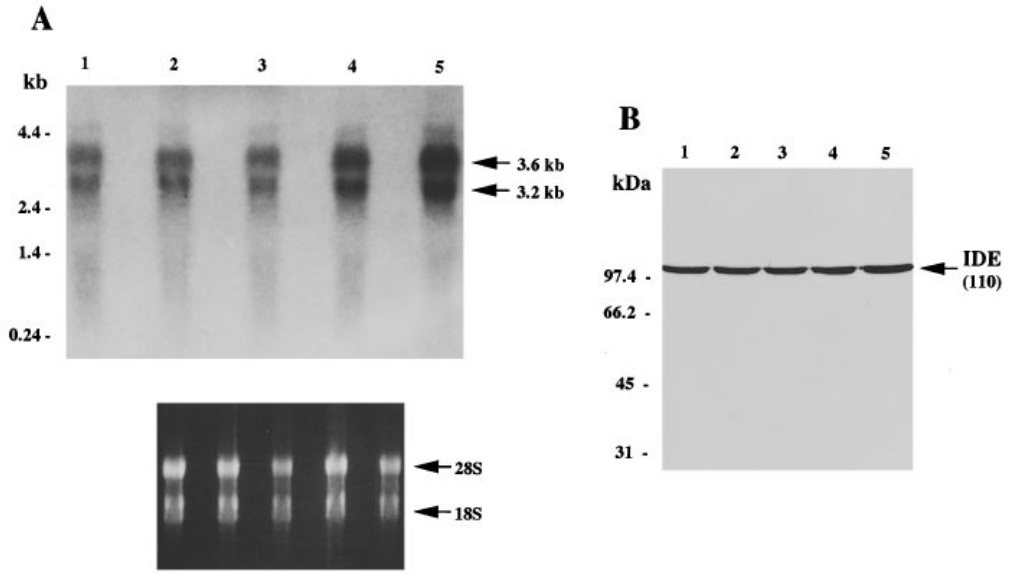

Figure 8 Effect of clofibrate and retinoic acid on the induction of IDE mRNA and IDE protein in HepG2 cells

(**A**) HepG2 cells were incubated in the absence (lanes 1 and 3) or in the presence of 0.01 mM retinoic acid (lane 2), 0.1 mM and 0.5 mM clofibrate (lanes 4 and 5, respectively), for a period of 6 days. Total cellular RNAs were then extracted using TRIzol and subjected to Northern blotting. The RNAs (20 μg) were resolved by electrophoresis on a denaturing formaldehyde/1% agarose gel, transferred by diffusion to nylon membranes, and hybridized with a 3.0 kb *Eco*RI restriction fragment of IDE cDNA probe labelled with [α-^{32}P]dCTP. A photograph of the stained gel is shown in the bottom panel, and the 28 S and 18 S ribosomal RNAs are indicated on the right. (**B**) HepG2 cell lysates (50 μg of protein per lane) from the same treated cells as in (**A**) were evaluated by immunoblotting for their content of IDE with the anti-IDE antibody 9B12; control cells (lanes 1 and 3), 0.01 mM retinoic acid (lane 2), 0.1 mM clofibrate (lane 4) and 0.5 mM clofibrate-treated cells (lane 5). Northern and Western blots are representative of four separate experiments.

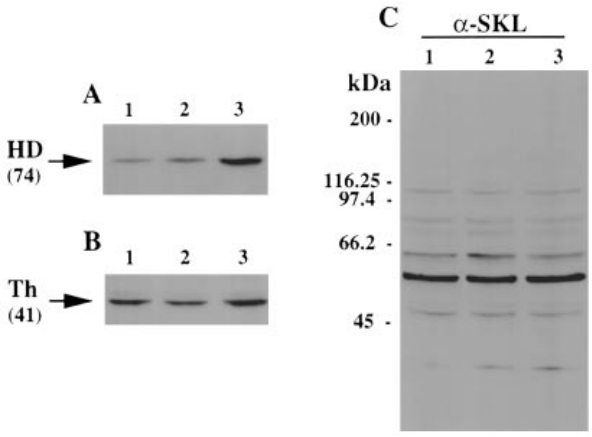

Figure 9 Effect of clofibrate and retinoic acid on the induction of type-I and -II peroxisomal proteins in HepG2 cells

HepG2 cells were incubated in the absence (lanes 1) or in the presence of 0.01 mM retinoic acid (lanes 2) and 0.5 mM clofibrate (lanes 3), for a period of 6 days as in Figure 8. Whole-cell lysates (20 μg of protein per lane) were evaluated by immunoblotting for their content of hydratase dehydrogenase (HD) (**A**), for their content of thiolase (Th) (**B**) and for their immunoreactivity with polyclonal antiserum to the type-I peroxisomal targeting motif SKL (**C**).

9B, lane 3) compared with control cells (Figures 9A and 9B, lanes 1). However, no effect was observed with retinoic acid treatment (Figures 9A and 9B, lanes 2). In addition, both treatments had no effect on the expression levels of type-I peroxisomal proteins reactive to antibodies specific to the type-I PTS SKL (Figure 9C).

DISCUSSION

IDE has usually been described as a cytoplasmic enzyme due to its recovery in the 100000 ***g*** supernatant after tissue homogenization and differential centrifugation [2,4,5]. However, both immunofluorescence [6,7] and immunocryoelectron microscopy [7] on stably transfected cells overexpressing IDE revealed a major peroxisomal labelling, while a minor diffuse labelling was also found in the cytosol. On the other hand, despite possessing the type-I PTS in its primary sequence, Western blots of rat liver subcellular fractions accounted for only a minority (about 10%) of the protease as peroxisomal, the majority of the protein being recovered in the cytosol [5]. We hypothesized that the variable recovery of IDE in cytosol results from one or more mechanisms, including: (i) the leakage of IDE from fragile peroxisomes during homogenization and the rigors of subcellular fractionation [22]; (ii) an artifact of overexpression which could influence the peroxisomal targeting of IDE; and (iii) the presence of a cytosolic cofactor(s) which could mask the type-I PTS [8].

To overcome some of the limitations encountered when purified peroxisomes are used, we have developed a digitonin-permeabilized cell system since digitonin treatment is known to be a mild procedure [13]. Digitonin permeabilization of Tran[^{35}S]-labelled and non-radiolabelled HepG2 cells unequivocally defined the highest concentration of IDE in the cytoplasm of non-transfected cells. Consequently, the variability of IDE levels found in cytosol after various technical procedures is unlikely to be due to the well known fragility of peroxisomes [22] or to an artifact of overexpression.

It is conceivable that the dual cytosolic and peroxisomal location of IDE may be cell-type specific and limited to cells expressing high levels of protein p70, the cytosolic protein physically associated with IDE. The failure to detect p70 in IDE

immunoprecipitates from radiolabelled control and stably transfected CHO cells overexpressing IDE (where the proteinase displays a minor cytoplasmic location [6,7]) supports this hypothesis. Based on the experiments carried out in this study, the association between IDE and p70 is concluded to be physiological due to: (i) the chemical cross-linking in the intact cell of IDE to a polypeptide of 70 kDa; (ii) the recovery in IDE immunoprecipitates from metabolically labelled cell lysates of a 70 kDa polypeptide; and (iii) the recovery in IDE immunoprecipitates from non-radiolabelled HepG2 cell lysates of two major Coomassie Blue-stained proteins corresponding to the 110 kDa IDE and 70 kDa p70 proteins. Immunological cross-reactivity between p70 and the well-characterized anti-IDE antibody 9B12 was ruled out as: (i) the antibody was found specifically to recognize by immunoblotting only a single protein of molecular mass 110 kDa (Figure 2A) as reported by us in our previous studies [5,6] and by others [15]; and (ii) the failure to co-immunoprecipitate p70 with IDE in sequential immunoprecipitations under denaturing conditions (Figure 2B).

Since both biochemical ([5]; this study) and morphological evaluations [6,7] of the subcellular distribution of IDE revealed a genuine cytosolic location for the peroxisomal protease, it is likely that IDE functions not only in peroxisomes. A dual cytosolic and peroxisomal location has also been observed for sterol carrier protein-2, another protein that possesses the peroxisomal targeting signal -AKL at its C-terminus, and the cytosolic location has been implicated in the functioning of this transport protein [23]. Also, a member of the epoxide hydrolase family having a putative type-I PTS (SKI) exists in both cytosolic and peroxisomal locations [24]. IDE has been proposed to be the main cellular clearance mechanism for insulin and glucagon polypeptides [3]. However, significant progress in understanding the physiological enzymes for insulin and glucagon degradation has recently toned down this postulated role [2,25], mainly based on the facts that: (i) overexpression of IDE has not unanimously been found to modify the rate of insulin degradation in intact cells [3,16]; (ii) IDE which displays a dual cytoplasmic and peroxisomal location is not readily available for internalized insulin and glucagon which are located within endosomes [2,5,26,27]; (iii) an acidic thiol-endopeptidase unrelated to IDE with an endosomal location and that fulfills the requirements for such an insulinase has been recently identified [5]; and (iv) membrane-associated cathepsins B and D are responsible for proteolysis of glucagon within hepatic endosomes [28,29].

Recently, the functional significance of peroxisome-associated IDE in degrading cleaved leader peptides of peroxisomal proteins targeted by the type-II PTS has been elucidated [6]. To test whether conditions that increase the level of the relevant substrates of peroxisome-associated IDE (the free type-II motif) upset the equilibrium by promoting translocation of cytosol-associated IDE to peroxisomes and/or modifying the rate of IDE synthesis, we have examined the subcellular distribution and the expression of the protease in HepG2 cells pretreated with clofibrate or retinoic acid, two drugs reported to induce peroxisomal proliferation [19,20]. Clofibrate treatment, which increased the expression of type-II peroxisomal enzymes such as hydratase dehydrogenase and thiolase, had no effect on the subcellular location of IDE as measured by digitonin-permeabilization studies. Northern-blot analysis of total mRNA from HepG2 cells allowed the identification of two human IDE mRNA species of 3.6 and 3.2 kb, the level of which was greatly increased by induction with clofibrate. However, the magnitude of induction of the human IDE transcripts was much greater than that of the IDE protein revealed by Western blotting. Such induction of IDE transcripts without parallel induction at the protein level is not unprecedented and has also been reported in stably transfected KMHL cells [7]. These differences suggest that the expression of IDE might be regulated post-transcriptionally. The peroxisomal proliferation caused by fibrate hypolipidaemic drugs partially results from a transcriptional induction of the enzymes of the β-oxidation pathway which is mediated by peroxisome proliferator-activated receptors (PPARs), members of the nuclear receptor superfamily [30]. PPARs regulate the expression of genes containing specific peroxisome proliferator response elements in their regulatory sequences [31]. Further experiments are required to test whether this sequence may be directly involved in the regulation of IDE gene expression by clofibrate.

In summary, we have identified a 70 kDa cytosolic protein which specifically binds IDE in hepatoma cells. Although the identity and physiological significance of p70 remain to be determined, its ability to be associated in *vivo* with IDE suggests that it may be involved in the mechanism by which the type-I peroxisomal protein IDE is retained within the cytoplasm of parenchymal liver cells. The availability of a purification protocol using co-immunoprecipitation under non-denaturing conditions should enable us to obtain sequence information on the p70 protein band and to elucidate the primary structure of the protein by cDNA cloning. This should allow us to gain novel insight(s) into the physiological significance of cytoplasm-associated IDE which until now has been unclear.

We thank Dr. John J. M. Bergeron (McGill University, Montréal, Canada) for generously supporting these studies. We thank Dr. Richard A. Roth (Stanford University, CA, U.S.A.) for the kind gifts of anti-IDE antibody 9B12, plasmid pIDE-F1.BS for IDE and the CHO cell line overexpressing IDE. We are grateful to Dr. Richard A. Rachubinski (University of Edmonton, Alberta, Canada) for polyclonal antisera to rat peroxisomal enzymes. We acknowledge Dr. Paul A. Walton (McGill University, Montréal, Canada) for gifts of anti-hsp70 antibodies. This work was supported by grants from the Institut National de la Santé et de la Recherche Médicale (F. A.).

REFERENCES

1 Rawlings, N. D. and Barrett, A. J. (1993) Biochem. J. **290**, 205–218
2 Authier, F., Posner, B. I. and Bergeron, J. J. M. (1994) in Cellular Proteolytic Systems (Ciechanover, A. and Schwartz, A. L., eds.), vol. 15, pp. 89–113, Wiley-Liss, Inc., New York
3 Becker, A. B. and Roth, R. A. (1995) Methods Enzymol. **248**, 693–703
4 Authier, F., Posner, B. I. and Bergeron, J. J. M. (1996) Clin. Invest. Med. **19**, 149–160
5 Authier, F., Rachubinski, R. A., Posner, B. I. and Bergeron, J. J. M. (1994) J. Biol. Chem. **269**, 3010–3016
6 Authier, F., Bergeron, J. J. M., Ou, W.-J., Rachubinski, R. A., Posner, B. I. and Walton, P. A. (1995) Proc. Natl. Acad. Sci. U.S.A. **92**, 3859–3863
7 Kuo, W.-L., Gehm, B. D., Rosner, M. R., Li, W. and Keller, G. (1994) J. Biol. Chem. **269**, 22599–22606
8 Rachubinski, R. A. and Subramani, S. (1995) Cell **83**, 525–528
9 Pierotti, A. R., Prat, A., Chesneau, V., Gaudoux, F., Leseney, A.-M., Foulon, T. and Cohen, P. (1994) Proc. Natl. Acad. Sci. U.S.A. **91**, 6078–6082
10 Braun, H.-P. and Schmitz, U. K. (1995) Trends Biochem. Sci. **20**, 171–175
11 VanderVere, P. S., Bennett, T. M., Oblong, J. E. and Lamppa, G. K. (1995) Proc. Natl. Acad. Sci. U.S.A. **92**, 7177–7181
12 Adames, N., Blundell, K., Ashby, M. N. and Boone, C. (1995) Science **270**, 464–467
13 Wendland, M. and Subramani, S. (1993) J. Cell Biol. **120**, 675–685
14 Bradford, M. M. (1976) Anal. Biochem. **72**, 248–254
15 Shii, K. and Roth, R. A. (1986) Proc. Natl. Acad. Sci. U.S.A. **83**, 4147–4151
16 Affholter, J. A., Hsieh, C.-L., Francke, U. and Roth, R. A. (1990) Mol. Endocrinol. **4**, 1125–1135
17 Walton, P. A., Wendland, M., Subramani, S., Rachubinski, R. A. and Welch, W. J. (1994) J. Cell Biol. **125**, 1037–1046
18 Ou, W.-J., Cameron, P. H., Thomas, D. Y. and Bergeron, J. J. M. (1993) Nature (London) **364**, 771–776
19 Hertz, R. and Bar-Tana, J. (1992) Biochem. J. **281**, 41–43
20 Rachubinski, R. A., Fujiki, Y., Mortensen, R. M. and Lazarow, P. B. (1984) J. Cell Biol. **99**, 2241–2246

21 Affholter, J. A., Fried, V. A. and Roth, R. A. (1988) Science **242**, 1415–1418
22 Alexson, S. E. H., Fujiki, Y., Shio, H. and Lazarow, P. B. (1985) J. Cell Biol. **101**, 294–305
23 Ossendorp, B. C. and Wirtz, K. W. A. (1993) Biochimie **75**, 191–200
24 Knehr, M., Thomas, H., Arand, M., Gebel, T., Zeller, H.-D. and Oesch, F. (1993) J. Biol. Chem. **268**, 17623–17627
25 Authier, F., Posner, B. I. and Bergeron, J. J. M. (1996) FEBS Lett. **389**, 55–60
26 Authier, F., Janicot, M., Lederer, F. and Desbuquois, B. (1990) Biochem. J. **272**, 703–712
27 Doherty, J. J., Kay, D. G., Lai, W. H., Posner, B. I. and Bergeron, J. J. M. (1990) J. Cell Biol. **110**, 35–42
28 Authier, F. and Desbuquois, B. (1991) Biochem. J. **280**, 211–218
29 Authier, F., Mort, J. S., Bell, A. W., Posner, B. I. and Bergeron, J. J. M. (1995) J. Biol. Chem. **270**, 15798–15807
30 Issemann, I. and Green, S. (1990) Nature (London) **347**, 645–650
31 Zhang, B., Marcus, S. L., Sajjadi, F. G., Alvares, K., Reddy, J. K., Subramani, S., Rachubinski, R. A. and Capone, J. P. (1992) Proc. Natl. Acad. Sci. U.S.A. **89**, 7541–7545

Receieved 11 March 1996/30 May 1996; accepted 25 June 1996